

# 000 001 002 003 004 005 006 007 008 009 010 011 012 013 014 015 016 017 018 019 020 021 022 023 024 025 026 027 028 029 030 031 032 033 034 035 036 037 038 039 040 041 042 043 044 045 046 047 048 049 050 051 052 053 DPARALLEL: LEARNABLE PARALLEL DECODING FOR DLLMS

Anonymous authors

Paper under double-blind review

## ABSTRACT

Diffusion large language models (dLLMs) have recently drawn considerable attention within the research community as a promising alternative to autoregressive generation, offering parallel token prediction and lower inference latency. Yet, their parallel decoding potential remains largely underexplored, as existing open-source models still require nearly token-length decoding steps to ensure performance. To address this, we introduce dParallel, a simple and effective method that unlocks the inherent parallelism of dLLMs for fast sampling. We identify that the key bottleneck to parallel decoding arises from the sequential certainty convergence for masked tokens. Building on this insight, we introduce the core of our approach: certainty-forcing distillation, a novel training strategy that distills the model to follow its original sampling trajectories while enforcing it to achieve high certainty on masked tokens more rapidly and in parallel. Extensive experiments across various benchmarks demonstrate that our method can dramatically reduce the number of decoding steps while maintaining performance. When applied to the LLaDA-8B-Instruct model, dParallel reduces decoding steps from 256 to 30 on GSM8K, achieving an 8.5 $\times$  speedup without performance degradation. On the MBPP benchmark, it cuts decoding steps from 256 to 24, resulting in a 10.5 $\times$  speedup while maintaining accuracy.

## 1 INTRODUCTION

Diffusion large language models (dLLMs) (Yu et al., 2025a; Zhang et al., 2025; Yi et al., 2024) have emerged as a promising alternative to autoregressive LLMs (Achiam et al., 2023; Bai et al., 2023). By leveraging bidirectional attention, they overcome the sequential generation bottleneck and enable parallel, random-order text generation, offering the potential for substantial improvements in inference efficiency. This potential has already been demonstrated in proprietary models such as Mercury (Labs et al., 2025), Gemini-Diffusion, and Seed-Diffusion (Song et al., 2025).

However, realizing this parallelism in existing open-source dLLMs remains challenging. Open implementations such as LLaDA (Nie et al., 2025; Zhu et al., 2025) and Dream (Ye et al., 2025), still require a number of decoding steps proportional to the sequence length to maintain generation quality, resulting in limited inference efficiency. Many recent efforts have attempted to accelerate dLLMs. Some approaches (Ma et al., 2025; Liu et al., 2025; Wu et al., 2025; Hu et al., 2025) reduce the time cost per decoding step by enabling KV caching. Other works (Israel et al., 2025; Wei et al., 2025; Li et al., 2025a;b; Gwak et al., 2025; Ben-Hamu et al., 2025) focus on optimizing parallel sampling algorithms to accelerate inference by reducing the necessary decoding steps. Despite these advancements, existing methods have yet to fully unlock the parallel potential of dLLMs, as highly parallel decoding consistently leads to degraded performance.

This paper focuses on training dLLMs to unleash their potential for parallel decoding. We identify the core bottleneck as their sequential certainty convergence. Although dLLMs predict all masked tokens in parallel at each step, the certainty of these predictions still converges in a left-to-right sequential order. This sequential propagation of certainty prevents the model from reliably determining multiple tokens simultaneously, forming the key bottleneck to highly parallel decoding. Employing naive teacher forcing or diffusion forcing (Chen et al., 2024) training is insufficient to resolve this issue, as they solely focus on trajectory alignment. Consequently, a new training paradigm centered on predictive certainty itself is needed for dLLMs to further unlock parallelism.

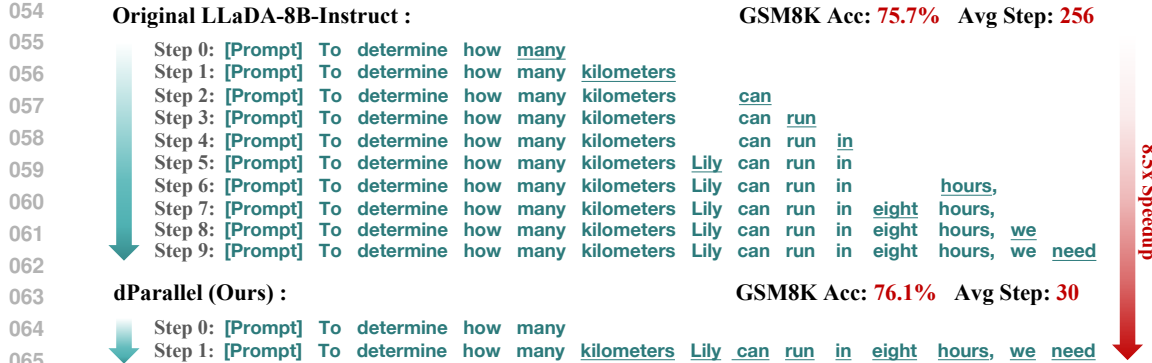


Figure 1: Our method achieves highly parallel decoding. Compared to the original LLaDA Model, dParallel decodes over 8 tokens per step on GSM8K while preserving the accuracy.

Building on this insight, we present certainty-forcing distillation, a simple and effective training strategy that directly leverages token certainty as a training signal. The core idea is to convert dLLM’s inherently sequential certainty propagation into a more parallel convergence process. Concretely, we guide a pretrained dLLM to self-distill along its original semi-autoregressive decoding trajectory to maintain trajectory consistency, while simultaneously minimizing its predictive entropy over correctly predicted masked tokens to enforce high certainty. Certainty-forcing enables more tokens to reach high certainty in parallel at each step, thereby significantly extending the boundary of parallel decoding in dLLMs.

We evaluate the effectiveness of our method on two representative open-source dLLMs: LLaDA, a native dLLM trained from scratch, and Dream, a dLLM initialized from an autoregressive LLM. Comprehensive experiments across multiple benchmarks demonstrate that our approach significantly reduces the number of decoding steps in dLLMs, while maintaining comparable performance. For instance, when applied to the LLaDA-8B-Instruct model, our approach achieves an 88% reduction in decoding steps on GSM8K (Cobbe et al., 2021), yielding an 8.5× speedup without sacrificing accuracy (Fig.1). On MBPP (Austin et al., 2021b), it further reduces decoding steps by 91%, delivering a 10.5× acceleration while maintaining performance. Furthermore, the training process of our method is highly efficient and low-cost. Leveraging Low-Rank Adaptation (LoRA) (Hu et al., 2022), the training can be completed in just 10 hours on only eight A5000 GPUs with 24 GB memory each.

In conclusion, we present dParallel, a learnable approach that unleashes the potential of parallel decoding in dLLMs, drastically reducing the number of decoding steps. Our analysis identifies the core bottleneck as the sequential convergence of certainty across masked tokens. To address this, we introduce a certainty-forcing distillation strategy that ensures consistency with the original generation trajectory while encouraging masked tokens to attain high certainty faster and more in parallel. Extensive experiments demonstrate the effectiveness of our method. This work establishes a new baseline and provides a foundation for future research on few-step and parallel dLLMs.

## 2 RELATED WORKS

**Diffusion Language Models.** In recent years, diffusion models (Ho et al., 2020; Song et al., 2020) have established dominance in the field of visual generation (Rombach et al., 2022; Podell et al., 2023; Ruiz et al., 2023; Zhang et al., 2023). However, their application to text generation remains highly challenging. Masked diffusion models (Shi et al., 2024; Austin et al., 2021a; Sahoo et al., 2024; Zheng et al., 2024; Lou et al., 2023) have emerged as a promising approach, modeling language in the discrete space by predicting masked tokens, thereby offering the potential for fast and parallel decoding. Building upon this idea, two representative dLLMs, LLaDA (Nie et al., 2025) and Dream (Ye et al., 2025), have recently attracted significant attention from the community, demonstrating that dLLMs can achieve performance comparable to autoregressive LLMs at the billion-parameter scale. Beyond these developments, there is also growing interest in reasoning dLLMs (Zhao et al.,

108 2025; Wang et al., 2025b; Zhu et al., 2025), multimodal dLLMs (You et al., 2025; Yu et al., 2025b;  
 109 Yang et al., 2025; Li et al., 2025c), and code generation (Gong et al., 2025; Xie et al., 2025) dLLMs.  
 110

111 **Accelerating Diffusion Language Models.** The potential of dLLMs in inference efficiency remains  
 112 largely underexplored. Recent studies have increasingly focused on accelerating the decoding pro-  
 113 cess of dLLMs. Some approaches (Ma et al., 2025; Liu et al., 2025; Wu et al., 2025; Hu et al.,  
 114 2025; Chen et al., 2025) aim to reduce the time cost for each decoding step by enabling caching  
 115 mechanisms and employing token dropping during inference. Other works (Israel et al., 2025; Wei  
 116 et al., 2025; Li et al., 2025a;b; Gwak et al., 2025; Ben-Hamu et al., 2025) focus on reducing the total  
 117 number of decoding steps by designing improved sampling strategies. In addition, hybrid methods  
 118 (Wang et al., 2025a; Arriola et al., 2025) have been proposed that combine the generative paradigms  
 119 of dLLMs and autoregressive LLMs, training models to realize more efficient inference pipelines.  
 120 SDTT Deschenaux & Gulcehre (2024) employs progressive distillation to reduce the inference steps.  
 121 Further effort Xu & Yang (2025) leverages quantization techniques to construct lightweight dLLMs.  
 122

### 123 3 PRELIMINARIES

124 **Masked Diffusion Language Models (MDLMs).** Unlike AR-LLMs that predict tokens in a strict  
 125 left-to-right fashion, MDLMs (Shi et al., 2024; Austin et al., 2021a; Zheng et al., 2024) formulate  
 126 generation as a probabilistic process consisting of a forward *masking* corruption and a reverse *de-  
 127 noising* recovery. The forward process corrupts a clean sequence  $x_0$  into  $x_t$  at level  $t \in [0, 1]$ :

$$128 \quad q(x_t | x_0) = \prod_{i=1}^L \left[ (1-t) \delta(x_t^i = x_0^i) + t \delta(x_t^i = [\text{MASK}]) \right]. \quad (1)$$

131 The reverse process is parameterized by a mask predictor  $p_\theta$ , which attempts to recover  $x_0$  from  $x_t$ .  
 132 At each step, the model predicts all masked tokens jointly:

$$134 \quad p_\theta(x_0 | x_t) = \prod_{i: x_t^i = [\text{MASK}]} p_\theta(x_0^i | x_t), \quad (2)$$

136 The training objective, defined as the negative log-likelihood restricted to masked positions, has  
 137 been shown to upper bound the model’s negative log-likelihood (Ou et al., 2024):  
 138

$$139 \quad \mathcal{L}(\theta) = -\mathbb{E}_{t, x_0, x_t} \left[ \frac{1}{t} \sum_{i=1}^L \mathbf{1}[x_t^i = [\text{MASK}]] \log p_\theta(x_0^i | x_t) \right]. \quad (3)$$

142 **Sampling Process.** Inference proceeds through a discretized reverse process: at each step the model  
 143 predicts distributions for all masked tokens in parallel, samples provisional tokens, and then applies  
 144 a dynamic remasking strategy to determine which positions remain masked for further refinement.  
 145 Unlike autoregressive decoding, this procedure allows multiple tokens to be determined in parallel,  
 146 thereby enabling more flexible and potentially faster generation.

## 147 4 METHOD

### 150 4.1 THE BARRIERS TO PARALLEL DECODING

152 Diffusion language models are designed, in principle, for highly parallel token prediction. Yet in  
 153 practice, this theoretical promise breaks down. To understand this discrepancy, we analyze the cer-  
 154 tainty dynamics of token predictions in dLLMs, revealing why their potential for parallel decoding  
 155 remains unrealized.

156 **Certainty Correlates with Prediction Accuracy.** We first establish that token-level certainty is  
 157 a reliable indicator of prediction correctness. Using LLaDA-8B-Instruct on the GSM8K test set  
 158 (Cobbe et al., 2021), we adopt a remasking strategy with varying confidence thresholds and record  
 159 the average determined confidence of tokens. Fig 2 (a) shows a strong positive correlation between  
 160 token confidence and the generation correctness: tokens resolved at higher confidence consistently  
 161 achieve higher accuracy, whereas low-confidence commitments lead to frequent errors. This result  
 162 confirms that high certainty is a necessary condition for accurate generation.

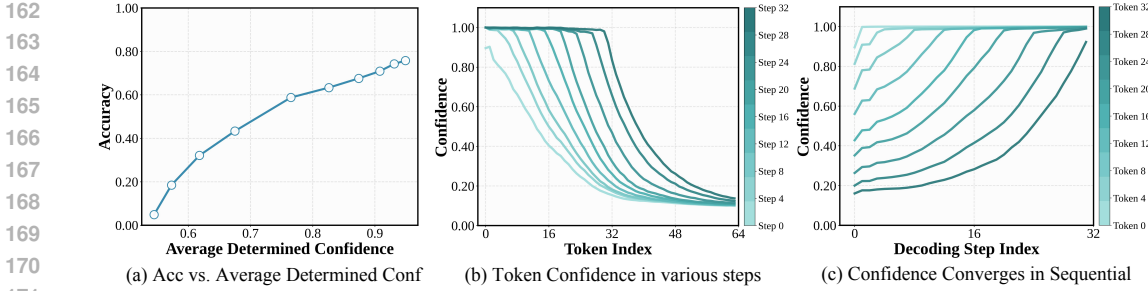


Figure 2: Empirical Studies: (a) The average confidence score exhibits a positive correlation with generation accuracy. (b) Token confidence propagates sequentially during the decoding process. (c) Convergence trajectories of confidence for different tokens.

**Certainty Converges to Peak Sequentially.** The high certainty is not achieved in parallel. Instead, it propagates sequentially through the sequence. At any given decoding step, the model predicts all masked tokens, but only a small subset, typically those adjacent to already known context, attain high confidence. The vast majority of tokens remain in a low-confidence regime until a new context becomes available. Once a confident token is committed, it provides a new conditioning context that allows another subset to rise in certainty at the next step.

This dynamic is illustrated in Fig 2 (b), which shows the average confidence of tokens progressing as a left-to-right propagation over decoding steps. Fig 2 (c) further confirms this at the individual token level, showing confidence trajectories that converge to high certainty in a staggered, sequential order. Together, these findings reveal that high certainty does not emerge in parallel but unfolds sequentially through iterative context enrichment.

**The Fundamental Bottleneck.** The key bottleneck is the sequential convergence of certainty. While true parallelism requires committing many tokens in a single step, a dLLM gains high certainty only for a few neighboring tokens per iteration. Forcing multiple commitments too early introduces low-confidence predictions, causing cascading errors and performance degradation.

**Key to Unlocking Parallelism Potential.** The above insight illuminates a clear path forward: if we could guide the model to achieve peak confidence in parallel across multiple token positions, we could break the sequential bottleneck. However, traditional training strategies, such as teacher forcing and diffusion forcing (Chen et al., 2024), are inadequate for this purpose, as their focus on trajectory alignment overlooks the dynamics of predictive certainty. Consequently, unlocking greater parallelism in dLLMs requires a new training paradigm that directly optimizes for certainty. We therefore propose certainty-forcing distillation, a novel strategy that reshapes the model’s certainty dynamics by using token certainty itself as a direct training signal.

## 4.2 CERTAINTY-FORCING DISTILLATION

We propose certainty-forcing distillation, a straightforward approach that enforces parallel certainty along the original trajectory without altering it. An overview is shown in Fig 3.

**Teacher Trajectory Generation.** Let  $M_{\theta_T}$  be the teacher model (a pre-trained vanilla dLLM), and let  $M_{\theta_S}$  be the student model, initialized as an identical copy. We train on a dataset  $\mathcal{D} = \{X^{(i)}\}_{i=1}^K$ , where each  $X^{(i)}$  is an instruction prompt. For each prompt, the teacher  $M_{\theta_T}$  generates a target response trajectory using a semi-autoregressive remasking strategy with total length  $L$  and block size  $L_b$ , producing a sequence  $Y = (y_1, y_2, \dots, y_L)$ . This sequence is partitioned into  $N$  contiguous blocks  $\{B_1, B_2, \dots, B_N\}$  such that  $L = N \times L_b$ , where the  $n$ -th block is defined as  $B_n = (y_{(n-1)L_b+1}, \dots, y_{nL_b})$  for  $n \in \{1, \dots, N\}$ .

**Semi-Autoregressive Forward Masking.** To simulate the trajectory generation process for training, we perturb the clean trajectory  $Y$  and create a noisy input sequence  $\tilde{Y}$  by applying a semi-autoregressive structural masking scheme. We first uniformly sample a block index  $n \sim \{0, \dots, N-1\}$ . The sequence is then divided into three distinct parts based on this index: (1) Context Blocks ( $i \leq nL_b$ ): Tokens within the first  $n$  blocks remain unmasked, serving as the model’s context. (2)

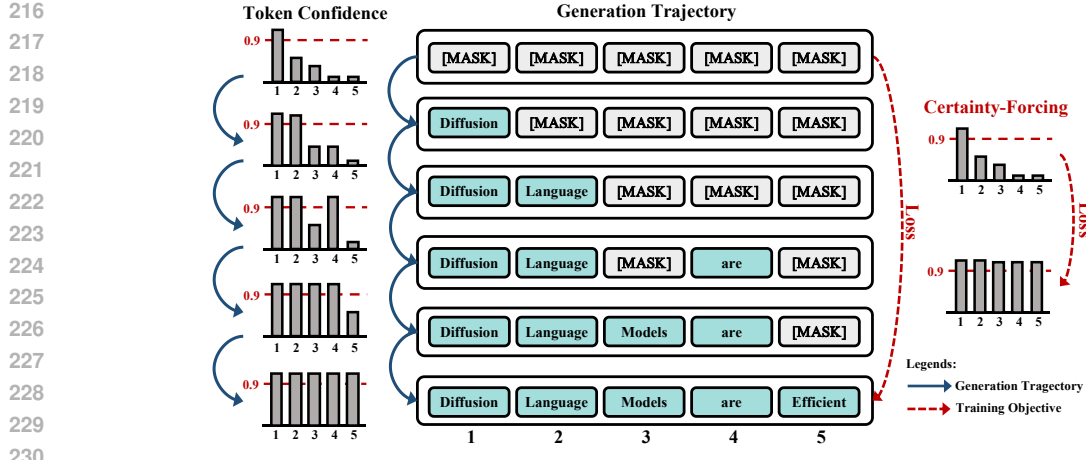


Figure 3: Overview of proposed certainty-forcing distillation. The dLLM is self-distilled along its original generation trajectory, ensuring consistency with the trajectory throughout training while encouraging token certainty to converge faster in parallel rather than sequentially.

Active Block ( $nL_b < i \leq (n+1)L_b$ ): This is the block currently being generated, where its tokens are randomly replaced by the token [MASK] with masking probability  $p_m = q$ . (3) Future Blocks ( $i > (n+1)L_b$ ): All tokens in subsequent blocks are fully masked, as they have not yet been generated. This procedure yields a noisy token  $\tilde{y}_i$  at each position  $i$ , defined as:

$$\tilde{y}_i = \begin{cases} y_i, & \text{if } i \leq nL_b \quad (\text{Context}) \\ \begin{cases} y_i & \text{with probability } 1 - q \\ [\text{MASK}] & \text{with probability } q \end{cases} & \text{if } nL_b < i \leq (n+1)L_b \quad (\text{Active Block}) \\ [\text{MASK}], & \text{if } i > (n+1)L_b \quad (\text{Future}) \end{cases} \quad (4)$$

The resulting sequence  $\tilde{Y}$  simulates an intermediate state in the semi-autoregressive generative process, where the model is predicting the  $(n+1)$ -th block given the context of the first  $n$  blocks.

**Training Objective.** Our objective differs from standard dLLM pre-training, which typically aims to predict all masked tokens across the sequence. Instead, we restrict the learning signal to the masked tokens within the active block  $B_{n+1}$ . Our training objective is for the student model not only to replicate the target sampling trajectory within the active block but also to parallel achieve maximal certainty in its predictions.

To enforce consistency between the student model's generated trajectory and that of the teacher, we apply standard Cross-Entropy (CE) loss on the masked tokens of the active block, denoted as  $\mathcal{M}_a$ :

$$\mathcal{L}_{\text{Consistency}} = -\frac{1}{|\mathcal{M}_a|} \sum_{i \in \mathcal{M}_a} \log p_{\theta}(y_i | \tilde{Y}), \quad (5)$$

where  $p_{\theta}(y_i | \tilde{Y})$  denotes the probability assigned by the student model to the correct token  $y_i$  at position  $i$ , conditioned on the noisy input sequence  $\tilde{Y}$ . However, conventional CE loss is insufficient for our certainty-maximizing target. It focuses solely on correctness, and once the correct token is predicted, the gradient quickly vanishes, offering no incentive to further increase confidence.

To explicitly encourage highly confident predictions, we introduce a term that directly minimizes the entropy of the model's output distribution, incorporating a temperature parameter  $T$ . This loss is applied only to the masked tokens in the active block that the student model already predicts correctly. Formally, we define the set of correctly predicted tokens as

$$\mathcal{M}_c = \left\{ i \in \mathcal{M}_a \mid \arg \max_{v \in \mathcal{V}} p_{\theta}(v | \tilde{Y}) = y_i \right\}, \quad (6)$$

---

270 **Algorithm 1** Certainty-Forcing Distillation (CFD)

---

271 **Require:** Teacher  $M_{\theta_T}$ , student  $M_{\theta_S}$ ; target trajectory set  $\mathcal{D} = \{Y^{(i)}\}_{i=1}^K$ ; temperature  $T > 0$ ;  
 272 weight  $\beta \geq 0$ ; optimizer  $\mathcal{O}$ ; token length  $L$ ; block length  $L_b$ ; mask ratio  $q \in (0, 1]$ .

273 **Notation:**  $H(p) = -\sum_{v \in \mathcal{V}} p(v) \log p(v)$

274 1: **for**  $j = 1 \dots \text{Iteration}$  **do**

275 2:   Sample  $Y \sim \mathcal{D}$ ,  $n \sim \{0, 1, \dots, L/L_b - 1\}$ ;

276 3:    $(\tilde{Y}, \mathcal{M}_a) \leftarrow \text{SEMI-AR-FOWARDMASKING}(Y, q, n, L, L_b)$ ;

277 4:    $z \leftarrow M_{\theta_S}(\tilde{Y})$ ;

278 5:    $p_i(v) \leftarrow \text{softmax}(z_i)_v$ ,  $p_i^{(T)}(v) \leftarrow \text{softmax}(z_i/T)_v$ ,  $\forall v \in \mathcal{V}$

279 6:    $\mathcal{L}_{\text{Consistency}} \leftarrow -|\mathcal{M}_a|^{-1} \sum_{i \in \mathcal{M}_a} \log p_i(y_i)$ ;

280 7:    $\mathcal{M}_c \leftarrow \{i \in \mathcal{M}_a \mid \arg \max_{v \in \mathcal{V}} p_i(v) = y_i\}$ ;

281 8:    $\mathcal{L}_{\text{Certainty}} \leftarrow \mathbf{1}[|\mathcal{M}_c| > 0] \cdot |\mathcal{M}_c|^{-1} \sum_{i \in \mathcal{M}_c} H(p_i^{(T)})$ ;

282 9:    $\mathcal{L}_{\text{CFD}} \leftarrow \mathcal{L}_{\text{Consistency}} + \beta \mathcal{L}_{\text{Certainty}}$ ;

283 10:    $\theta_S \leftarrow \mathcal{O}(\theta_S, \nabla_{\theta_S} \mathcal{L}_{\text{CFD}})$ ;

284 11: **end for**

---

285

286

287 where  $\mathcal{V}$  denotes the vocabulary. The certainty-forcing loss is then defined as the average entropy of  
 288 the predictive distributions for these tokens:

$$\mathcal{L}_{\text{Certainty}} = \frac{1}{|\mathcal{M}_c|} \sum_{i \in \mathcal{M}_c} \left( -\sum_{v \in \mathcal{V}} p_{\theta}(v \mid \tilde{Y}; T) \log p_{\theta}(v \mid \tilde{Y}; T) \right), \quad (7)$$

292 where  $p_{\theta}(v \mid \tilde{Y}; T)$  denotes the temperature-scaled softmax distribution. Minimizing this term  
 293 encourages the student model to generate sharper, higher-certainty distributions over the correct  
 294 tokens, where  $T$  controls the strength of the certainty enforcement.

295 The overall training objective is a combination of consistency loss and the certainty-forcing loss:

$$\mathcal{L}_{\text{CFD}} = \mathcal{L}_{\text{Consistency}} + \beta \mathcal{L}_{\text{Certainty}}, \quad (8)$$

298 where  $\beta$  is a hyperparameter balancing the objective of matching the teacher’s trajectory with the  
 299 objective of enforcing high certainty. We find that this simple distillation strategy significantly  
 300 accelerates the parallel convergence of certainty in dLLMs, thereby unlocking their inherent potential  
 301 for parallel decoding. The overall training pipeline is summarized in Algorithm 1

## 303 5 EXPERIMENTS

### 305 5.1 EXPERIMENTAL SETUP

307 **Implementation Details.** We evaluate the effectiveness of our method on two representative open-  
 308 source dLLMs: LLaDA-8B-Instruct (Nie et al., 2025) and Dream-7B-Instruct (Ye et al., 2025). The  
 309 training is conducted using the LoRA technique (Hu et al., 2022). For semi-autoregressive masking,  
 310 we set the block length to  $L_b = 32$  for LLaDA and  $L_b = 256$  for Dream, with a fixed masking  
 311 ratio of 50%. The certainty loss is applied with a temperature of  $T = 0.5$ . Full training config-  
 312urations are provided in the appendix. During inference, our models adopt an entropy-threshold  
 313 semi-autoregressive remasking strategy, which is inherently consistent with our training objective.

314 **Training Data.** As a self-distillation approach, we use prompts from publicly available training  
 315 datasets and let the pretrained model generate its own responses as training data. For LLaDA-  
 316 8B-Instruct, we sample prompts from the GSM8K (Cobbe et al., 2021), PRM12K (Lightman  
 317 et al., 2023) training set, and part of the Numina-Math dataset (Li et al., 2024). Using a semi-  
 318 autoregressive strategy with a sequence length of 256 and block length of 32, we generate about  
 319 100k target trajectories. For Dream-7B-Instruct, we adopt the same trajectory generation strategy,  
 320 and additionally generate code data using prompts from a subset of the AceCode dataset (about 10k)  
 321 (Zeng et al., 2025). We further filter out responses containing incorrect answers. Importantly, all  
 322 training tokens are generated by the model itself, without introducing any external data as targets.

323 **Evaluation Details.** We evaluate our models across multiple benchmarks, including two mathe-  
 324 matics datasets (GSM8K and MATH (Lewkowycz et al., 2022)) and two code generation datasets

324  
 325 Table 1: Evaluation results on LLaDA-8B-Instruct. For all methods, we adopt a semi-autoregressive  
 326 remasking strategy with a total sequence length of 256 and a block length of 32. For our approach,  
 327 the entropy threshold is set to either 0.45 or 0.5 for different tasks.

Benchmark	Method	#Steps ↓	Latency↓	Speedup ↑	Accuracy↑
<b>GSM8K</b> -CoT (0-shot)	LLaDA-8B-Instruct	256	18.6s	1.0×	75.7%
	Dual-Cache	256	9.7s	1.9×	72.9%
	Few-step Decoding	64	4.7s	4.0×	68.6%
	Conf-threshold Decoding	72	5.2s	3.6×	75.5%
	Consistency Distillation	64	4.7s	4.0×	69.9%
	<b>dParallel (Ours)</b>	<b>30</b>	<b>2.2s</b>	<b>8.5×</b>	<b>76.1%</b>
<b>MATH</b> (4-shot)	LLaDA-8B-Instruct	256	50.9s	1.0×	33.5%
	Dual-Cache	256	11.3s	4.5×	32.6%
	Few-step Decoding	64	12.7s	4.0×	26.3%
	Conf-threshold Decoding	97	17.6s	2.9×	33.2%
	Consistency Distillation	64	12.7s	4.0×	28.0%
	<b>dParallel (Ours)</b>	<b>46</b>	<b>8.9s</b>	<b>5.7×</b>	<b>31.5%</b>
<b>HumanEval</b> (0-shot)	LLaDA-8B-Instruct	256	23.5s	1.0×	38.4%
	Dual-Cache	256	9.8s	2.4×	34.1%
	Few-step Decoding	64	5.9s	4.0×	19.5%
	Conf-threshold Decoding	77	6.7s	3.5×	37.2%
	Consistency Distillation	64	5.9s	4.0×	19.5%
	<b>dParallel (Ours)</b>	<b>33</b>	<b>2.9s</b>	<b>8.2×</b>	<b>40.2%</b>
<b>MBPP</b> (3-shot)	LLaDA-8B-Instruct	256	50.1s	1.0×	42.4%
	Dual-Cache	256	10.7s	4.7×	39.8%
	Few-step Decoding	64	12.5s	4.0×	19.6%
	Conf-threshold Decoding	68	12.8s	3.9×	41.6%
	Consistency Distillation	64	12.5s	4.0×	25.0%
	<b>dParallel (Ours)</b>	<b>24</b>	<b>4.8s</b>	<b>10.5×</b>	<b>40.8%</b>

351 (HumanEval (Chen et al., 2021) and MBPP (Austin et al., 2021b)). For GSM8K, we append a  
 352 chain-of-thought (CoT) prompt (Wei et al., 2022) after each question. We report accuracy, the av-  
 353 erage number of decoding steps, latency, and speedup ratio to provide a comprehensive evaluation.  
 354 All efficiency evaluations are conducted on NVIDIA RTX 6000 Ada GPUs.

355 **Baselines.** We evaluate the original dLLM under its official default inference setting, and further  
 356 compare our approach with four baselines that seek to accelerate the generation: (1) Dual-Cache:  
 357 enable KV-cache on both prefix tokens and suffix tokens (Wu et al., 2025). (2) Few-step Decoding:  
 358 reducing the number of decoding steps used by the original dLLM. (3) Conf-threshold Decoding:  
 359 apply adaptive remasking based on the model’s confidence in predicting masked tokens (Wu et al.,  
 360 2025; Yu et al., 2025b), with the confidence threshold set as 0.90 or 0.95 depending on the task.  
 361 (4) Consistency Distillation: training the dLLM to predict all remaining masked tokens from inter-  
 362 mediate state along its own generation trajectory (Luo et al., 2023). The training data and LoRA  
 363 configuration are the same as our method.

## 365 5.2 MAIN RESULTS

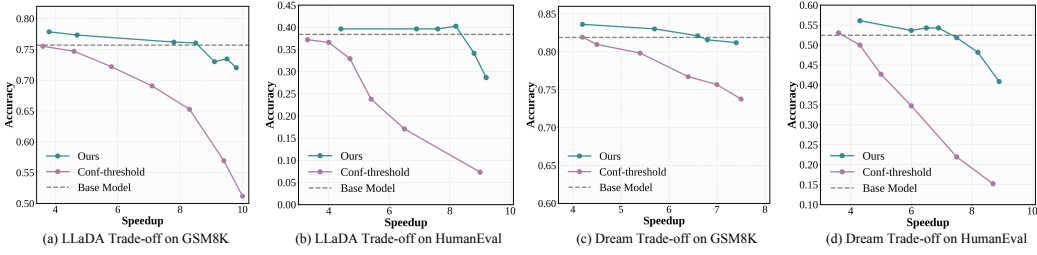
367 **Results on the Native LLaDA Model.** As shown in Table 1, directly reducing the decoding steps  
 368 of the original model leads to a substantial drop in performance. Consistency distillation has only  
 369 a marginal effect on LLaDA, offering a slight improvement over the original model under the same  
 370 number of steps. The confidence-threshold remasking strategy preserves accuracy, but its paral-  
 371 lelism is limited, averaging only 3–4 tokens decoded per step. In contrast, our method significantly  
 372 pushes the boundaries of parallel inference in dLLMs, achieving more than 8 tokens decoded per  
 373 step on average while still maintaining performance. Notably, for LLaDA, we trained using only  
 374 prompts from mathematical tasks, yet the model still exhibited a remarkable improvement in paral-  
 375 lel decoding ability on code tasks.

376 **Results on the AR-initialized Dream Model.** As shown in Table 2, our method also demonstrates  
 377 superior performance on the Dream model, which is initialized from an AR-LLM. Compared to  
 other approaches designed to reduce the number of decoding steps, dParallel achieves a substan-

378

379  
380  
381  
Table 2: Evaluation results on Dream-8B-Instruct. The original model uses the official inference  
setting with a sequence length of 256. Other methods adopt semi-autoregressive remasking with the  
same length and a block size of 32. The entropy threshold for our method is set to either 0.45 or 0.5.

Benchmark	Method	#Steps ↓	Latency ↓	Speedup ↑	Accuracy↑
<b>GSM8K</b> -CoT (0-shot)	Dream-7B-Instruct	256	17.2s	1.0×	82.9%
	Dual-Cache	256	8.2s	2.1×	79.5%
	Few-step Decoding	64	4.3s	4.0×	59.0%
	Conf-threshold Decoding	61	4.0s	4.3×	81.9%
	Consistency Distillation	64	4.3s	4.0×	75.6%
	<b>dParallel (Ours)</b>	<b>39</b>	<b>2.5s</b>	<b>6.9×</b>	82.1%
<b>MATH</b> (0-shot)	Dream-7B-Instruct	256	17.5s	1.0×	39.5%
	Dual-Cache	256	8.2s	2.1×	38.8%
	Few-step Decoding	64	4.4s	4.0×	16.7%
	Conf-threshold Decoding	93	6.1s	2.9×	38.9%
	Consistency Distillation	64	4.4s	4.0×	29.6%
	<b>dParallel (Ours)</b>	<b>63</b>	<b>4.1s</b>	<b>4.2×</b>	38.3%
<b>HumanEval</b> -Instruct (0-shot)	Dream-7B-Instruct	256	25.9s	1.0×	52.4%
	Dual-Cache	256	8.4s	3.1×	47.0%
	Few-step Decoding	64	6.5s	4.0×	16.5%
	Conf-threshold Decoding	71	7.3s	3.5×	53.1%
	Consistency Distillation	64	6.4s	4.0×	34.2%
	<b>dParallel (Ours)</b>	<b>37</b>	<b>3.8s</b>	<b>6.9×</b>	54.3%
<b>MBPP</b> -Instruct (0-shot)	Dream-7B-Instruct	256	19.8s	1.0×	58.8%
	Dual-Cache	256	8.9s	2.2×	52.8%
	Few-step Decoding	64	5.0s	4.0×	25.0%
	Conf-threshold Decoding	43	3.3s	5.9×	56.4%
	Consistency Distillation	64	5.0s	4.0×	37.4%
	<b>dParallel (Ours)</b>	<b>29</b>	<b>2.2s</b>	<b>8.8×</b>	56.2%

404  
405  
406  
407  
408  
409  
410  
411  
412  
Figure 4: Comparison of speed–accuracy trade-off curves between confidence-threshold decoding  
413 and our method. (a) and (b) show results on the LLaDA model for GSM8K and HumanEval, respec-  
414 tively. (c) and (d) present results on the Dream model for GSM8K and HumanEval benchmarks.  
415416  
417 tially higher speedup while maintaining accuracy, thereby greatly enhancing decoding parallelism.  
418 It is worth noting that we observed a risk of degeneration toward the original AR LLM when train-  
419 ing Dream with semi-autoregressive masking. To avoid this issue, we employed standard random  
420 masking over the entire sequence instead. Consequently, the acceleration gains of our method on  
421 Dream are slightly lower than those observed on LLaDA.422  
423 **Superior Efficiency–Performance Trade-off.** In Fig 4, we compare our method against the original  
424 model with confidence-threshold decoding in terms of the efficiency–performance trade-off curve.  
425 Our approach achieves a substantially better trade-off. On LLaDA with GSM8K, at the same 9.4×  
426 speedup, our method attains 16.5% higher accuracy than confidence-threshold decoding. On Hu-  
427 manEval, at the same 9.3× speedup, our method improves accuracy by 21.3%. Results on Dream  
428 exhibit a similar curve. These findings strongly demonstrate that our method effectively broadens  
429 the boundary of parallel decoding in diffusion language models.430  
431 **Faster and Parallel Certainty Convergence.** As illustrated in Fig 5, the original dLLM exhibits  
432 a sequential convergence of token certainty, where each step produces high confidence only for a  
433 small set of neighboring tokens, while the majority remain in a low-confidence range. Confidence-  
434 based decoding can extend the boundary of token certainty but still follows a sequential propagation

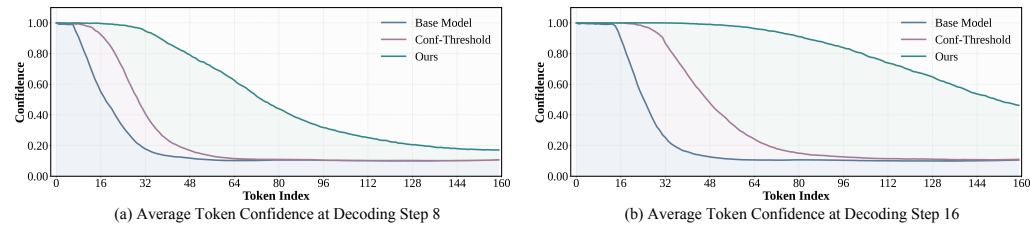


Figure 5: Average token confidence at the 8th and 16th decoding steps for LLaDA-8B-Instruct Model on GSM8K. The proposed certainty-forcing strategy reshapes the original sequential certainty convergence into a faster and more parallel convergence process.

Table 3: Ablation study on different training strategies of our method using the LLaDA model.

Consistency Loss	Certainty Loss	Semi-AR Masking	GSM8K-CoT (0-shot)			HumanEval (0-shot)		
			#Steps ↓	Speed ↑	Acc ↑	#Steps ↓	Speed ↑	Acc ↑
✓		✓	53	4.5x	73.5%	71	3.6x	36.0%
	✓	✓	23	10.4x	57.8%	28	9.8x	30.5%
✓	✓		44	5.5x	73.3%	61	4.3x	32.9%
✓	✓	✓	30	8.5x	76.1%	33	8.2x	40.2%

pattern. In contrast, our dParallel, trained with certainty-forcing distillation, transforms this process into a significantly faster and more parallel convergence of certainty. Such parallel convergence further unlocks the potential of dLLMs for highly efficient parallel decoding.

### 5.3 ABLATION STUDY

**Ablation Study on Training Strategy.** We conducted an ablation study to validate the effectiveness of our proposed certainty-forcing distillation, with the results shown in Table 3. When the certainty-forcing loss is removed, the remaining consistency loss is insufficient to alter the sequential convergence pattern of the dLLM, resulting in speed and performance similar to the baseline model. Conversely, applying only the certainty loss without enforcing trajectory consistency achieves high decoding speed but leads to a sharp performance drop. Finally, our use of semi-autoregressive forward masking effectively aligns the trajectory generation process with self-distillation, yielding superior efficiency and performance. These results collectively demonstrate that each component in the training process is essential.

**Ablation Study on Masking Ratio.** We conduct an ablation study to determine the optimal masking ratio, training LLaDA for one epoch with various settings as shown in Table 4. We find that a fixed masking ratio of 50% yields the best performance, offering significant acceleration while preserving accuracy. In contrast, both higher and lower fixed ratios, as well as random ratios, lead to a noticeable accuracy degradation. This suggests that a 50% ratio creates an optimal trade-off between the training signals for consistency and certainty by balancing masked and unmasked tokens. Importantly, training with this fixed ratio does not impair the model’s ability to handle variable ratios during inference.

## 6 CONCLUSION

In this paper, we present dParallel, a simple yet effective method that unleashes the parallel decoding potential of dLLMs. At the core of our approach is certainty-forcing distillation, a novel training strategy that maintains trajectory consistency while compelling high-certainty predictions, thus overcoming the sequential certainty propagation issue. Extensive experiments across various benchmarks validate the effectiveness of our method. Our work establishes a new baseline for parallel decoding in dLLMs and explores a new avenue for dLLM training paradigms.

Table 4: Performance of our method applied to LLaDA-8B-Instruct on GSM8K with different masking ratios used in the forward process during training.

Masking Ratio	#Steps ↓	Speed ↑	Acc ↑
Random	36	7.1x	72.4%
25%	35	7.3x	69.9%
75%	38	6.7x	73.7%
100%	31	8.3x	71.1%
<b>50%</b>	<b>36</b>	<b>7.1x</b>	<b>76.3%</b>

486 REFERENCES  
487

488 Josh Achiam, Steven Adler, Sandhini Agarwal, Lama Ahmad, Ilge Akkaya, Florencia Leoni Ale-  
489 man, Diogo Almeida, Janko Altenschmidt, Sam Altman, Shyamal Anadkat, et al. Gpt-4 technical  
490 report. *arXiv preprint arXiv:2303.08774*, 2023.

491 Marianne Arriola, Aaron Gokaslan, Justin T Chiu, Zhihan Yang, Zhixuan Qi, Jiaqi Han, Sub-  
492 ham Sekhar Sahoo, and Volodymyr Kuleshov. Block diffusion: Interpolating between autore-  
493 gressive and diffusion language models. *arXiv preprint arXiv:2503.09573*, 2025.

494 Jacob Austin, Daniel D Johnson, Jonathan Ho, Daniel Tarlow, and Rianne Van Den Berg. Structured  
495 denoising diffusion models in discrete state-spaces. *Advances in neural information processing*  
496 systems, 34:17981–17993, 2021a.

497 Jacob Austin, Augustus Odena, Maxwell Nye, Maarten Bosma, Henryk Michalewski, David Dohan,  
498 Ellen Jiang, Carrie Cai, Michael Terry, Quoc Le, et al. Program synthesis with large language  
499 models. *arXiv preprint arXiv:2108.07732*, 2021b.

500 Jinze Bai, Shuai Bai, Yunfei Chu, Zeyu Cui, Kai Dang, Xiaodong Deng, Yang Fan, Wenbin Ge,  
501 Yu Han, Fei Huang, et al. Qwen technical report. *arXiv preprint arXiv:2309.16609*, 2023.

502 Heli Ben-Hamu, Itai Gat, Daniel Severo, Niklas Nolte, and Brian Karrer. Accelerated sampling from  
503 masked diffusion models via entropy bounded unmasking. *arXiv preprint arXiv:2505.24857*,  
504 2025.

505 Boyuan Chen, Diego Martí Monsó, Yilun Du, Max Simchowitz, Russ Tedrake, and Vincent Sitz-  
506 mann. Diffusion forcing: Next-token prediction meets full-sequence diffusion. *Advances in*  
507 *Neural Information Processing Systems*, 37:24081–24125, 2024.

508 Mark Chen, Jerry Tworek, Heewoo Jun, Qiming Yuan, Henrique Ponde de Oliveira Pinto, Jared  
509 Kaplan, Harri Edwards, Yuri Burda, Nicholas Joseph, Greg Brockman, Alex Ray, Raul Puri,  
510 Gretchen Krueger, Michael Petrov, Heidy Khlaaf, Girish Sastry, Pamela Mishkin, Brooke Chan,  
511 Scott Gray, Nick Ryder, Mikhail Pavlov, Alethea Power, Lukasz Kaiser, Mohammad Bavarian,  
512 Clemens Winter, Philippe Tillet, Felipe Petroski Such, Dave Cummings, Matthias Plappert, Fotios  
513 Chantzis, Elizabeth Barnes, Ariel Herbert-Voss, William Hebgen Guss, Alex Nichol, Alex  
514 Paino, Nikolas Tezak, Jie Tang, Igor Babuschkin, Suchir Balaji, Shantanu Jain, William Saunders,  
515 Christopher Hesse, Andrew N. Carr, Jan Leike, Josh Achiam, Vedant Misra, Evan Morikawa, Alec  
516 Radford, Matthew Knight, Miles Brundage, Mira Murati, Katie Mayer, Peter Welinder, Bob Mc-  
517 Grew, Dario Amodei, Sam McCandlish, Ilya Sutskever, and Wojciech Zaremba. Evaluating large  
518 language models trained on code. 2021.

519 Xinhua Chen, Sitao Huang, Cong Guo, Chiyue Wei, Yintao He, Jianyi Zhang, Hai Li, Yiran  
520 Chen, et al. Dpad: Efficient diffusion language models with suffix dropout. *arXiv preprint*  
521 *arXiv:2508.14148*, 2025.

522 Karl Cobbe, Vineet Kosaraju, Mohammad Bavarian, Mark Chen, Heewoo Jun, Lukasz Kaiser,  
523 Matthias Plappert, Jerry Tworek, Jacob Hilton, Reiichiro Nakano, et al. Training verifiers to  
524 solve math word problems. *arXiv preprint arXiv:2110.14168*, 2021.

525 Justin Deschenaux and Caglar Gulcehre. Beyond autoregression: Fast llms via self-distillation  
526 through time. *arXiv preprint arXiv:2410.21035*, 2024.

527 Shansan Gong, Ruixiang Zhang, Huangjie Zheng, Jiatao Gu, Navdeep Jaitly, Lingpeng Kong, and  
528 Yizhe Zhang. Diffucoder: Understanding and improving masked diffusion models for code gen-  
529 eration. *arXiv preprint arXiv:2506.20639*, 2025.

530 Daehoon Gwak, Minseo Jung, Junwoo Park, Minho Park, ChaeHun Park, Junha Hyung, and Jaegul  
531 Choo. Reward-weighted sampling: Enhancing non-autoregressive characteristics in masked dif-  
532 fusion llms. *arXiv preprint arXiv:2509.00707*, 2025.

533 Jonathan Ho, Ajay Jain, and Pieter Abbeel. Denoising diffusion probabilistic models. *Advances in*  
534 *neural information processing systems*, 33:6840–6851, 2020.

540 Edward J Hu, Yelong Shen, Phillip Wallis, Zeyuan Allen-Zhu, Yuanzhi Li, Shean Wang, Lu Wang,  
 541 Weizhu Chen, et al. Lora: Low-rank adaptation of large language models. *ICLR*, 1(2):3, 2022.  
 542

543 Zhanqiu Hu, Jian Meng, Yash Akhauri, Mohamed S Abdelfattah, Jae-sun Seo, Zhiru Zhang, and  
 544 Udit Gupta. Accelerating diffusion language model inference via efficient kv caching and guided  
 545 diffusion. *arXiv preprint arXiv:2505.21467*, 2025.

546 Daniel Israel, Guy Van den Broeck, and Aditya Grover. Accelerating diffusion llms via adaptive  
 547 parallel decoding. *arXiv preprint arXiv:2506.00413*, 2025.

548 Inception Labs, Samar Khanna, Siddhant Kharbanda, Shufan Li, Harshit Varma, Eric Wang, Sawyer  
 549 Birnbaum, Ziyang Luo, Yanis Miraoui, Akash Palrecha, et al. Mercury: Ultra-fast language  
 550 models based on diffusion. *arXiv preprint arXiv:2506.17298*, 2025.

551

552 Aitor Lewkowycz, Anders Andreassen, David Dohan, Ethan Dyer, Henryk Michalewski, Vinay Ra-  
 553 masesh, Ambrose Sloane, Cem Anil, Imanol Schlag, Theo Gutman-Solo, et al. Solving quantitative  
 554 reasoning problems with language models. *Advances in neural information processing systems*,  
 555 35:3843–3857, 2022.

556 Jia Li, Edward Beeching, Lewis Tunstall, Ben Lipkin, Roman Soletskyi, Shengyi Huang, Kashif  
 557 Rasul, Longhui Yu, Albert Q Jiang, Ziju Shen, et al. Numinamath: The largest public dataset in  
 558 ai4maths with 860k pairs of competition math problems and solutions. *Hugging Face repository*,  
 559 13(9):9, 2024.

560

561 Jinsong Li, Xiaoyi Dong, Yuhang Zang, Yuhang Cao, Jiaqi Wang, and Dahua Lin. Beyond fixed:  
 562 Variable-length denoising for diffusion large language models. *arXiv e-prints*, pp. arXiv–2508,  
 563 2025a.

564 Pengxiang Li, Yefan Zhou, Dilxat Muhtar, Lu Yin, Shilin Yan, Li Shen, Yi Liang, Soroush Vosoughi,  
 565 and Shiwei Liu. Diffusion language models know the answer before decoding. *arXiv preprint*  
 566 *arXiv:2508.19982*, 2025b.

567

568 Shufan Li, Konstantinos Kallidromitis, Hritik Bansal, Akash Gokul, Yusuke Kato, Kazuki Kozuka,  
 569 Jason Kuen, Zhe Lin, Kai-Wei Chang, and Aditya Grover. Lavida: A large diffusion language  
 570 model for multimodal understanding. *arXiv preprint arXiv:2505.16839*, 2025c.

571 Hunter Lightman, Vineet Kosaraju, Yuri Burda, Harrison Edwards, Bowen Baker, Teddy Lee, Jan  
 572 Leike, John Schulman, Ilya Sutskever, and Karl Cobbe. Let's verify step by step. In *The Twelfth  
 573 International Conference on Learning Representations*, 2023.

574

575 Zhiyuan Liu, Yicun Yang, Yaojie Zhang, Junjie Chen, Chang Zou, Qingyuan Wei, Shaobo Wang,  
 576 and Linfeng Zhang. dllm-cache: Accelerating diffusion large language models with adaptive  
 577 caching. *arXiv preprint arXiv:2506.06295*, 2025.

578

579 Aaron Lou, Chenlin Meng, and Stefano Ermon. Discrete diffusion language modeling by estimating  
 the ratios of the data distribution. 2023.

580

581 Simian Luo, Yiqin Tan, Longbo Huang, Jian Li, and Hang Zhao. Latent consistency models: Synthe-  
 582 sizing high-resolution images with few-step inference. *arXiv preprint arXiv:2310.04378*, 2023.

583

584 Xinyin Ma, Runpeng Yu, Gongfan Fang, and Xincho Wang. dkv-cache: The cache for diffusion  
 585 language models. *arXiv preprint arXiv:2505.15781*, 2025.

586

587 Shen Nie, Fengqi Zhu, Zebin You, Xiaolu Zhang, Jingyang Ou, Jun Hu, Jun Zhou, Yankai  
 588 Lin, Ji-Rong Wen, and Chongxuan Li. Large language diffusion models. *arXiv preprint*  
 589 *arXiv:2502.09992*, 2025.

590

591 Jingyang Ou, Shen Nie, Kaiwen Xue, Fengqi Zhu, Jiacheng Sun, Zhenguo Li, and Chongxuan  
 592 Li. Your absorbing discrete diffusion secretly models the conditional distributions of clean data.  
 593 *arXiv preprint arXiv:2406.03736*, 2024.

594

595 Dustin Podell, Zion English, Kyle Lacey, Andreas Blattmann, Tim Dockhorn, Jonas Müller, Joe  
 596 Penna, and Robin Rombach. Sdxl: Improving latent diffusion models for high-resolution image  
 597 synthesis. *arXiv preprint arXiv:2307.01952*, 2023.

594 Robin Rombach, Andreas Blattmann, Dominik Lorenz, Patrick Esser, and Björn Ommer. High-  
 595 resolution image synthesis with latent diffusion models. In *Proceedings of the IEEE/CVF confer-  
 596 ence on computer vision and pattern recognition*, pp. 10684–10695, 2022.

597

598 Nataniel Ruiz, Yuanzhen Li, Varun Jampani, Yael Pritch, Michael Rubinstein, and Kfir Aberman.  
 599 Dreambooth: Fine tuning text-to-image diffusion models for subject-driven generation. In *Pro-  
 600 ceedings of the IEEE/CVF conference on computer vision and pattern recognition*, pp. 22500–  
 601 22510, 2023.

602 Subham Sahoo, Marianne Arriola, Yair Schiff, Aaron Gokaslan, Edgar Marroquin, Justin Chiu,  
 603 Alexander Rush, and Volodymyr Kuleshov. Simple and effective masked diffusion language  
 604 models. *Advances in Neural Information Processing Systems*, 37:130136–130184, 2024.

605

606 Jiaxin Shi, Kehang Han, Zhe Wang, Arnaud Doucet, and Michalis Titsias. Simplified and general-  
 607 ized masked diffusion for discrete data. *Advances in neural information processing systems*, 37:  
 608 103131–103167, 2024.

609 Jiaming Song, Chenlin Meng, and Stefano Ermon. Denoising diffusion implicit models. *arXiv  
 610 preprint arXiv:2010.02502*, 2020.

611

612 Yuxuan Song, Zheng Zhang, Cheng Luo, Pengyang Gao, Fan Xia, Hao Luo, Zheng Li, Yuehang  
 613 Yang, Hongli Yu, Xingwei Qu, et al. Seed diffusion: A large-scale diffusion language model with  
 614 high-speed inference. *arXiv preprint arXiv:2508.02193*, 2025.

615 Xu Wang, Chenkai Xu, Yijie Jin, Jiachun Jin, Hao Zhang, and Zhijie Deng. Diffusion llms can do  
 616 faster-than-ar inference via discrete diffusion forcing. *arXiv preprint arXiv:2508.09192*, 2025a.

617

618 Yinjie Wang, Ling Yang, Bowen Li, Ye Tian, Ke Shen, and Mengdi Wang. Revolutioniz-  
 619 ing reinforcement learning framework for diffusion large language models. *arXiv preprint  
 620 arXiv:2509.06949*, 2025b.

621 Jason Wei, Xuezhi Wang, Dale Schuurmans, Maarten Bosma, Fei Xia, Ed Chi, Quoc V Le, Denny  
 622 Zhou, et al. Chain-of-thought prompting elicits reasoning in large language models. *Advances in  
 623 neural information processing systems*, 35:24824–24837, 2022.

624

625 Qingyan Wei, Yaojie Zhang, Zhiyuan Liu, Dongrui Liu, and Linfeng Zhang. Accelerating dif-  
 626 fusion large language models with slowfast: The three golden principles. *arXiv preprint  
 627 arXiv:2506.10848*, 2025.

628 Chengyue Wu, Hao Zhang, Shuchen Xue, Zhijian Liu, Shizhe Diao, Ligeng Zhu, Ping Luo, Song  
 629 Han, and Enze Xie. Fast-dllm: Training-free acceleration of diffusion llm by enabling kv cache  
 630 and parallel decoding. *arXiv preprint arXiv:2505.22618*, 2025.

631

632 Zhihui Xie, Jiacheng Ye, Lin Zheng, Jiahui Gao, Jingwei Dong, Zirui Wu, Xueliang Zhao, Shansan  
 633 Gong, Xin Jiang, Zhenguo Li, et al. Dream-coder 7b: An open diffusion language model for  
 634 code. *arXiv preprint arXiv:2509.01142*, 2025.

635 Chen Xu and Dawei Yang. Dllmquant: Quantizing diffusion-based large language models. *arXiv  
 636 preprint arXiv:2508.14090*, 2025.

637

638 Ling Yang, Ye Tian, Bowen Li, Xinchen Zhang, Ke Shen, Yunhai Tong, and Mengdi Wang. Mmada:  
 639 Multimodal large diffusion language models. *arXiv preprint arXiv:2505.15809*, 2025.

640

641 Jiacheng Ye, Zhihui Xie, Lin Zheng, Jiahui Gao, Zirui Wu, Xin Jiang, Zhenguo Li, and Lingpeng  
 642 Kong. Dream 7b: Diffusion large language models. *arXiv preprint arXiv:2508.15487*, 2025.

643 Qiuhua Yi, Xiangfan Chen, Chenwei Zhang, Zehai Zhou, Linan Zhu, and Xiangjie Kong. Diffusion  
 644 models in text generation: a survey. *PeerJ Computer Science*, 10:e1905, 2024.

645

646 Zebin You, Shen Nie, Xiaolu Zhang, Jun Hu, Jun Zhou, Zhiwu Lu, Ji-Rong Wen, and Chongxuan  
 647 Li. Llada-v: Large language diffusion models with visual instruction tuning. *arXiv preprint  
 648 arXiv:2505.16933*, 2025.

648 Runpeng Yu, Qi Li, and Xinchao Wang. Discrete diffusion in large language and multimodal models:  
649 A survey. *arXiv preprint arXiv:2506.13759*, 2025a.  
650

651 Runpeng Yu, Xinyin Ma, and Xinchao Wang. Dimple: Discrete diffusion multimodal large language  
652 model with parallel decoding. *arXiv preprint arXiv:2505.16990*, 2025b.  
653

654 Huaye Zeng, Dongfu Jiang, Haozhe Wang, Ping Nie, Xiaotong Chen, and Wenhui Chen. Acecoder:  
655 Acing coder rl via automated test-case synthesis. *ArXiv*, abs/2207.01780, 2025.  
656

657 Lingzhe Zhang, Liancheng Fang, Chiming Duan, Minghua He, Leyi Pan, Pei Xiao, Shiyu Huang,  
658 Yunpeng Zhai, Xuming Hu, Philip S Yu, et al. A survey on parallel text generation: From parallel  
659 decoding to diffusion language models. *arXiv preprint arXiv:2508.08712*, 2025.  
660

661 Lvmin Zhang, Anyi Rao, and Maneesh Agrawala. Adding conditional control to text-to-image  
662 diffusion models. In *Proceedings of the IEEE/CVF international conference on computer vision*,  
663 pp. 3836–3847, 2023.  
664

665 Siyan Zhao, Devaansh Gupta, Qinqing Zheng, and Aditya Grover. d1: Scaling reasoning in diffusion  
666 large language models via reinforcement learning. *arXiv preprint arXiv:2504.12216*, 2025.  
667

668 Kaiwen Zheng, Yongxin Chen, Hanzi Mao, Ming-Yu Liu, Jun Zhu, and Qinsheng Zhang. Masked  
669 diffusion models are secretly time-agnostic masked models and exploit inaccurate categorical  
670 sampling. *arXiv preprint arXiv:2409.02908*, 2024.  
671

672

673

674

675

676

677

678

679

680

681

682

683

684

685

686

687

688

689

690

691

692

693

694

695

696

697

698

699

700

701

## APPENDIX

## A MORE IMPLEMENTATION DETAILS

In Table 5, we present the training configuration used for the certainty-forcing distillation process. For data generated by LLaDA-8B-Instruct (Nie et al., 2025) and LLaDA-1.5 (Zhu et al., 2025), we standardized sequence lengths by padding or truncating with the end-of-sequence token to a fixed length of 384 tokens. In contrast, for Dream-7B-Instruct (Ye et al., 2025), we preserved the original response length of 256 tokens per sample without modification. Additionally, we set the balance weight  $\beta = 2$  for all training.

Our training was conducted on two NVIDIA H100 GPUs, with a per-GPU mini-batch size of 1 and a gradient accumulation step of 32, resulting in an effective global batch size of 64. Notably, despite the relatively large model sizes, the adoption of parameter-efficient fine-tuning (PEFT) (Hu et al., 2022) and the use of shorter sequence lengths kept the memory footprint remarkably low. The entire training process required only 23 GB of GPU memory, meaning that it can be efficiently reproduced even on multiple consumer-grade GPUs with 24 GB of memory each. This efficiency highlights the practicality of our approach, as it enables large-scale distillation training to be carried out on widely accessible hardware rather than being restricted to specialized high-memory accelerators.

Table 5: The training configuration for certainty-forcing distillation across three base models.

Base Model	LoRA Rank	LoRA Alpha	Learning Rate	Lr-Schedule	Batchsize	Epoch
LLaDA-8B-Instruct	32	32	2e-5	constant	64	6
LLaDA-1.5	128	128	2e-5	constant	64	4
Dream-7B-Instruct	16	16	2e-5	cosine	64	3

Table 6: Evaluation results on LLaDA-1.5 Model across four benchmarks.

Benchmark	Method	#Steps $\downarrow$	Latency $\downarrow$	Speedup $\uparrow$	Accuracy $\uparrow$
<b>GSM8K</b> (0-shot)	LLaDA-8B-Instruct	256	19.1s	1.0 $\times$	76.0%
	<b>dParallel (Ours)</b>	<b>30</b>	<b>2.3s</b>	<b>8.5<math>\times</math></b>	76.3%
<b>MATH</b> (4-shot)	LLaDA-8B-Instruct	256	50.0s	1.0 $\times$	34.0%
	<b>dParallel (Ours)</b>	<b>45</b>	<b>8.7s</b>	<b>5.7<math>\times</math></b>	32.1%
<b>HumanEval</b> (0-shot)	LLaDA-8B-Instruct	256	22.0s	1.0 $\times$	41.5%
	<b>dParallel (Ours)</b>	<b>46</b>	<b>4.0s</b>	<b>5.6<math>\times</math></b>	40.2%
<b>MBPP</b> (3-shot)	LLaDA-8B-Instruct	256	49.0s	1.0 $\times$	43.2%
	<b>dParallel (Ours)</b>	<b>26</b>	<b>5.1s</b>	<b>9.8<math>\times</math></b>	41.6%

## B MORE EXPERIMENTAL RESULTS

In Table 6, we report the performance of applying our method to the LLaDA-1.5 model. Extensive evaluations across four standard benchmarks demonstrate the strong effectiveness of our approach on this reinforcement learning based model. Specifically, we reduce the original 256 decoding steps required by the baseline model to only 26–46 steps. This dramatic compression of the decoding steps delivers substantial acceleration in generation speed, while at the same time preserving accuracy and reliability across tasks.

In Figure 6, we present the average token confidence of the LLaDA-8B-Instruct model on GSM8K, measured across the first 160 positions over the initial 16 decoding steps. The results reveal that the original dLLM exhibits a clear sequential convergence of token certainty: each step yields high confidence for only a narrow band of neighboring tokens, while the majority remain in a low-confidence range. Although confidence-based decoding can extend the certainty frontier, it still follows this sequential propagation pattern. By contrast, our proposed dParallel, trained with certainty-forcing distillation, reshapes this process into a substantially faster and more parallel convergence of certainty. This parallel convergence further unlocks the efficiency potential of dLLMs, enabling highly parallel decoding.

756 **C CASE STUDY**  
757758 We also present additional case studies in Figure 7, Figure 8, and Figure 9. Our dParallel achieves  
759 significantly reduced decoding steps while maintaining the generation quality.  
760761 **D LIMITATIONS AND FUTURE WORK**  
762763 The primary limitation of our method is its reliance on the performance of the pretrained dLLM.  
764 While our approach achieves substantial gains in inference efficiency by unleashing the potential of  
765 parallel decoding and maintains strong accuracy, it cannot significantly improve the performance if  
766 the base model itself is weak.  
767768 As a next step, we plan to extend our certainty-forcing strategy to the pretraining stage of dLLMs  
769 and substantially scale up the training data to explore the performance boundary of our approach.  
770 Currently, we have only used a relatively small dataset of around 10k math problems. We believe  
771 that by dramatically increasing both the size and diversity of the training data, our method can  
772 yield further improvements: not only activating highly parallel decoding, but also enhancing overall  
773 model performance and demonstrating stronger generalization.  
774775 **E ETHICS STATEMENT**  
776777 This work adheres to the ICLR Code of Ethics. Our study does not involve human subjects or  
778 sensitive personal data. All datasets used are publicly available and properly licensed. While our  
779 method focuses on improving the efficiency of diffusion language models, we recognize potential  
780 risks of misuse in harmful applications and encourage responsible use aligned with ethical and legal  
781 standards.  
782783 **F REPRODUCIBILITY STATEMENT**  
784785 We have made significant efforts to ensure the reproducibility of our work. Detailed descriptions of  
786 model architectures, training objectives, and experimental settings are provided in the main text and  
787 Appendix. All datasets used are publicly available, and their preprocessing steps are documented in  
788 the main paper and appendix. Additionally, we include pseudocode and implementation details to  
789 facilitate replication, and source code is provided in the supplementary materials.  
790791 **G THE USE OF LARGE LANGUAGE MODELS**  
792793 In this paper, we only use large language models to correct grammar and spelling errors.  
794  
795  
796  
797  
798  
799  
800  
801  
802  
803  
804  
805  
806  
807  
808  
809

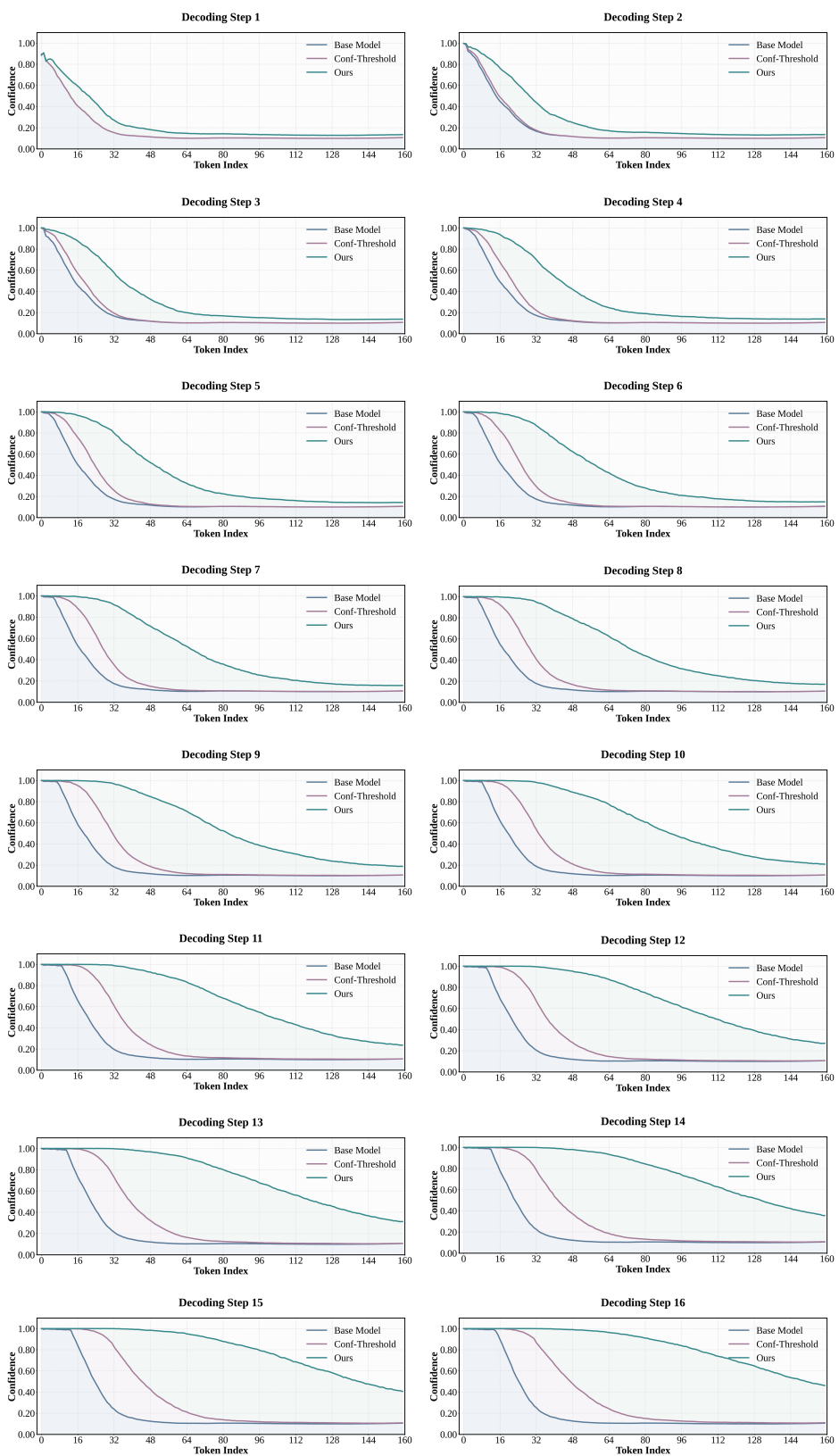


Figure 6: Average token confidence over the first 160 tokens across the first 16 decoding steps of the LLaDA-8B-Instruct model on GSM8K. Our certainty-forcing strategy transforms the sequential certainty convergence of the baseline into a faster and more parallel convergence process.

864  
865  
866  
867  
868  
869  
870

871 **Prompt:** Lily can run 12 kilometers per hour for 4 hours. After that, she runs 6 kilometers per hour. How many kilometers  
872 can she run in 8 hours? Please reason step by step, and put your final answer within `\boxed{}`.  
873

874 <b>LLaDA-8B-Instruct</b>	875 <b># 256 Decoding Steps</b>	876 <b>dParallel (Ours)</b>	877 <b># 28 Decoding Steps</b>
	To determine how many kilometers Lily can run in 8 hours, we need to break down the problem into two parts: the distance she runs in the first 4 hours and the distance she runs in the next 4 hours.		To determine how many kilometers Lily can run in 8 hours, we need to calculate the distance she covers in each segment of her run and then sum these distances.
878	First, let's calculate the distance she runs in the first 4 hours:	1. <b>**Calculate the distance run in the first 4 hours:**</b>	
879	- She runs at a speed of 12 kilometers per hour for 4 hours.	- Speed: 12 kilometers per hour	
880	- Distance = Speed $\times$ Time	- Time: 4 hours	
	- Distance = $12 \text{ km/h} \times 4 \text{ hours} = 48 \text{ km}$	- Distance: Speed $\times$ Time = $12 \text{ km/h} \times 4 \text{ hours} = 48 \text{ kilometers}$	
881	Next, let's calculate the distance she runs in the next 4 hours:	2. <b>**Calculate the distance run in the next 4 hours:**</b>	
882	- She runs at a speed of 6 kilometers per hour for 4 hours.	- Speed: 6 kilometers per hour	
883	- Distance = Speed $\times$ Time	- Time: 4 hours	
	- Distance = $6 \text{ km/h} \times 4 \text{ hours} = 24 \text{ km}$	- Distance: Speed $\times$ Time = $6 \text{ km/h} \times 4 \text{ hours} = 24 \text{ kilometers}$	
884	Now, we add the distances from both parts to find the total distance she can run in 8 hours:	3. <b>**Sum the distances from both segments:**</b>	
885	- Total distance = Distance in the first 4 hours + Distance in the next 4 hours	- Total distance = Distance in the first 4 hours + Distance in the next 4 hours	
886	- Total distance = $48 \text{ km} + 24 \text{ km} = 72 \text{ km}$	- Total distance = $48 \text{ km} + 24 \text{ km} = 72 \text{ kilometers}$	
887			
888	Therefore, the total distance Lily can run in 8 hours is <code>\boxed{72}</code> kilometers.	Therefore, the total distance Lily can run in 8 hours is <code>\boxed{72}</code> .	
889			

890 **Prompt:** Natalia sold clips to 48 of her friends in April, and then she sold half as many clips in May. How many clips did  
891 Natalia sell altogether in April and May? Please reason step by step, and put your final answer within `\boxed{}`.  
892

893 <b>LLaDA-8B-Instruct</b>	894 <b># 256 Decoding Steps</b>	895 <b>dParallel (Ours)</b>	896 <b># 30 Decoding Steps</b>
	To determine the total number of clips Natalia sold in April and May, we need to follow these steps:		To determine the total number of clips Natalia sold in April and May, we need to follow these steps:
897	1. Identify the number of clips Natalia sold in April.	1. <b>**Calculate the number of clips sold in May:**</b>	
898	2. Calculate the number of clips Natalia sold in May.	- Natalia sold clips to friends in May.	
	3. Add the number of clips sold in April and May to find the total.	- She sold half as many clips in May as she did in April.	
899	Step 1: Identify the number of clips Natalia sold in April. Natalia sold 48 clips in April.	- Since she sold 48 clips in April: - Therefore, the number of clips sold in May is $\lfloor \frac{48}{2} \rfloor = 24$ .	
900	Step 2: Calculate the number of clips Natalia sold in May. Natalia sold half as many clips in May as she did in April. Therefore, we calculate the number of clips sold in May as follows: $\lfloor \text{Number of clips sold in May} \rfloor = \frac{48}{2} = 24$	2. <b>**Calculate the total number of clips sold in both months:**</b>	
901	Step 3: Add the number of clips sold in April and May to find the total. We add the number of clips sold in April and May: $\lfloor \text{Total number of clips sold} \rfloor = 48 + 24 = 72$	- Add the number of clips sold in April to the number of clips sold in May. - Total clips sold = Clips sold in April + Clips sold in May - Total clips sold = $48 + 24$ - Total clips sold = 72	
902	Thus, the total number of clips Natalia sold in April and May is <code>\boxed{72}</code> .	Thus, the total number of clips Natalia sold in April and May is <code>\boxed{72}</code> .	
903			

910 **Figure 7:** Case study on LLaDA-8B-Instruct Model with chain-of-thought reasoning problem.  
911

912  
913  
914  
915  
916  
917

Figure 8: Case study on LLaDA-8B-Instruct Model with naive code generation task.

**Prompt:** Write a function to check if the given number is woodball or not..

LLaDA-8B-Instruct	# 256 Decoding Steps	dParallel (Ours)	# 49 Decoding Steps
<p>To determine if a given number is a "woodball," we need to define what a "woodball" is. For the sake of this example, let's assume a "woodball" is a number that is a multiple of 3. Here's a simple function in Python to check if a given number is a "woodball":</p> <pre>```python def is_woodball(number):     """     Check if the given number is a 'woodball' (i.e., a multiple of 3).      Parameters:     number (int): The number to check.      Returns:     bool: True if the number is a 'woodball', False otherwise.     """     return number % 3 == 0  # Example usage: print(is_woodball(9)) # True print(is_woodball(5)) # False ```  <p>In this function, `is_woodball`, we use the modulus operator `'%` to check if the number is divisible by 3. If the number is divisible by 3 with no remainder, it is a "woodball," and the function returns 'True'. Otherwise, it returns 'False'.</p></pre>		<p>Sure, I can help you with that. A woodball is a number that is a multiple of both 3 and 5. Here's a Python function to check if a given number is a woodball:</p> <pre>```python def is_woodball(number):     # Check if the number is a multiple of both 3 and 5     if number % 3 == 0 and number % 5 == 0:         return True     else:         return False  # Example usage: print(is_woodball(15)) # Output: True print(is_woodball(30)) # Output: True print(is_woodball(10)) # Output: False print(is_woodball(17)) # Output: False ```  <p>This function checks if the number is divisible by both 3 and 5 using the modulus operator `'%'. If both conditions are met, it returns 'True', indicating that the number is a woodball. Otherwise, it returns 'False'.</p></pre>	

Figure 9: Case study on LLaDA-8B-Instruct Model with instruction-based code generation task.